

Electrochemical Properties of Barium Cerate Doped with Zinc for Methanol Oxidation

¹Naveed Kausar Janjua*, ¹Mahwish Jabeen, ¹Mehrosh Islam, ¹Azra Yaqub, ²Sana Sabahat, ¹Sadia Mehmood, ¹Misbah Mumtaz, ¹Ayesha Mujtaba, ³Rizwan Raza, ²Ghazanfer Abbas
¹Department of Chemistry, Quaid-i-Azam University, Islamabad-45230, Pakistan.
²Department of Physics, COMSATS IIT, Park Road, Chak Shahzad, Islamabad-44000, Pakistan.
³Department of Physics COMSATS Institute of Information Technology, Lahore, Pakistan.
nkausarjanjua@yahoo.com*

Dedicated to Prof. Dr. John T. S. Irvine

(Received on 2nd September 2014, accepted in revised form 27th April 2015)

Summary: Barium cerate and its zinc doped series, BaCe_{1-x}Zn_xO₃ with 0.02 ≤ x ≤ 0.16, were synthesized using ammonia as a co-precipitant. The influence of zinc on phase and morphology was characterized using XRD and SEM, respectively. XRD revealed orthorhombic crystallinity for x= 0 to 14 mol% but distorted hexagonal phase for x = 16 mol%. SEM images revealed homogeneity of synthesized powders. The synthesized materials were then tested for their function as electrocatalyst for model analyte, methanol. Methanol electro-oxidation in acidic media was studied by modifying platinum electrode with BaCeO₃ materials using cyclic voltammetry. Kinetic (k_{s,b}, D_o) and thermodynamic parameters (E_a, ΔG, ΔH, ΔS) were estimated for methanol electrooxidation. The deduced value of diffusion coefficient of order of 10⁻¹⁰ cm²s⁻¹ indicated faster kinetics of methanol oxidation using BaCeO₃ than zinc doped sample in H₂SO₄ medium. The increasing temperature and methanol concentration enhanced the peak currents which pointed to the suitability of these materials as electrocatalysts. The stability and catalytic activity of these materials at various temperatures also aided to their potentiality in PEMFC application.

Key words: Zinc doped BaCeO₃; SEM; XRD; Methanol oxidation; Cyclic voltammetry; Thermodynamics.

Introduction

To meet energy demands across the globe, different energy harvesting ways are very crucial. The limited amount of fossil fuels and increasing energy demands emphasize the use of cheaper and environmental friendly energy technologies. There has been renewed interest in fuel cell technology. Fuel cell is primarily an energy convertor directly providing electricity by extracting chemical energy of a fuel [1, 2]. Among fuel cells, direct methanol fuel cells (DMFCs) are considered as promising power sources for portable electronic devices owing to low operational temperature, high energy density, simple construction, and environmental benignity. The methanol oxidation is one of the key reactions in DMFCs where it is oxidized to carbon dioxide at the anode.

To date, Pt has been found to be the most active catalyst towards methanol oxidation reaction (MOR). The electrochemical oxidation of methanol to CO₂ is governed by 6 electron process as shown by the equation:

$$\text{CH}_3\text{OH} + \text{H}_2\text{O} \rightarrow \text{CO}_2 + 6\text{H}^+ + 6\text{e}^- \quad (E^\circ = 0.02 \text{ V}), [3].$$

In this process, the soluble intermediates are continuously being formed at anode and their formation has been demonstrated

experimentally by various techniques like FTIR, liquid chromatography. These intermediates adsorbed onto the Pt electrode and reduce its active area. The electrode poisoning by adsorbed species (CO and CH_nO) decreases the catalytic activity of Pt towards MOR and thus affects the methanol fuel cell efficiency. Considering the high cost of Pt and its poisoning, the most important challenge is to find the ideal catalyst that promotes the oxidation of fuel and to develop low-temperature synthetic route for these fuel cells. To deal with this, platinum electrodes modified with perovskites have gained much popularity.

Perovskites having general formula A^{II}B^{IV}O₃ like barium cerate, barium zirconate, and strontium cerate where A and B are cations of different charges have got attention in this regard. BaCeO₃ (BCO) poses high conductivity but this material is chemically unstable in CO₂ rich atmosphere [4, 5]. Barium cerate properties can be modified by changing its stoichiometry or by doping with impurities [6, 7]. It has been found in literature that partial substitution of cerium by a dopant improves the conductivity as well as sufficient chemical and thermal stability over a wide range of conditions relevant to fuel cell operation.

*To whom all correspondence should be addressed.

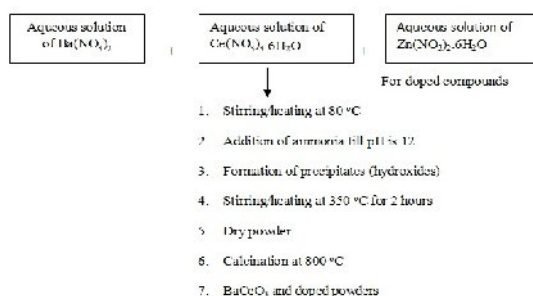
BaCeO₃ and its analogues have found a key position in material research of perovskites for particularly use as hydrogen sensor and proton conductor and their electronic and ionic conductivities offer a versatile role in fuel cell technology [6, 7].

In the present work, we report the synthesis and characterization of BaCeO₃ and its Zn doped analogues. Wet chemical method [8-12] was used to synthesize micro scale perovskite oxides with fine homogeneity of particles and controlled particle size. Pure barium cerate and its doped samples with different concentrations of zinc (BaCe_{1-x}Zn_xO₃) with x = 0.0 to 0.16 were synthesized through ammonia co-precipitation [13, 14] method and were characterized by XRD, FTIR, and SEM techniques. Drop casting technique is a simple method in which specific volume of suspension of electrocatalytic material is deposited on working electrode after ultrasonication in a suitable solvent. After depositing, binder is added to it so that active material gets bound to the working electrode [15, 16]. The electrochemical properties were tested by modifying Pt electrode with these synthesized samples using drop casting technique. To understand the electrocatalytic behavior of barium cerate and its analogues, study of kinetic and thermodynamic parameters is important which was done in the present scheme of work. To our knowledge, this study is the first time report on the applications of barium cerates as in proton exchange membrane fuel cells (PEMFC) type technology.

Experimental

Synthesis of pure BaCeO₃ and zinc doped powders

Synthesis process of pure BaCeO₃ nanoparticles and zinc doped barium cerate (BaCe_{1-x}Zn_xO₃) powders is shown in scheme 1.



Scheme-1: Flow chart showing steps involved in synthesis of pure barium cerate and zinc doped barium cerates (BaCe_{1-x}Zn_xO₃) by co-precipitation method.

Starting materials were Ba(NO₃)₂ (Sigma-Aldrich), Ce(NO₃)₃.6H₂O (Sigma-Aldrich) and Zn(NO₃)₂.6H₂O (Sigma-Aldrich). The appropriate molar ratio of precursors was mixed separately each in 50 ml of deionized water by continuous stirring at 80 °C until transparent solutions were obtained. These solutions were dissolved together and concentrated ammonia (Sigma Aldrich) was added to this mixture until yellowish precipitates formed at pH 11-12. During ammonia addition, solution was stirred continuously without heating. The precipitates were then dried on hot plate under stirring at 300 °C. Fumes were emitted during this stage, indicating the emission of nitrates. Finally, the precipitates were heated at 350 °C in furnace for spontaneous combustion. Then powdered sample obtained was sintered at 800 °C for 2 hours. Zinc doped series was also fabricated by similar method. The calcined powder obtained was then mechanically ground with acetone to ensure thorough mixing and get uniform particles. The BaCeO₃ and zinc doped barium cerate powders are coded as shown in Table-2.

Table-2: The studied samples with molecular formula, codes, and formula weight.

Formula	Sample code	Formula wt. (g mol ⁻¹)
BaCeO ₃	BCO	325
BaCe _{0.98} Zn _{0.02} O ₃	BCZO-1	324
BaCe _{0.96} Zn _{0.04} O ₃	BCZO-2	323
BaCe _{0.94} Zn _{0.06} O ₃	BCZO-3	321
BaCe _{0.92} Zn _{0.08} O ₃	BCZO-4	319
BaCe _{0.90} Zn _{0.10} O ₃	BCZO-5	318
BaCe _{0.88} Zn _{0.12} O ₃	BCZO-6	316
BaCe _{0.86} Zn _{0.14} O ₃	BCZO-7	315
BaCe _{0.84} Zn _{0.16} O ₃	BCZO-8	313

Electrode Preparation

The incorporation of noble metals like silver, gold and platinum wires or meshes as interconnects for electron transport might be helpful for their specific catalytic activity in modern fuel cell technologies. Also platinum (Pt) or glassy carbon modified with Pt nanoparticles act as a reproducible signal possessing electrode for electrooxidation of alcohols [17, 18]. These materials possess efficient and stable signal during the oxidation of methanol [19]. A high accessible surface area and support in electron transfer process makes Pt a better choice to be used as working electrode for electrochemical studies. Bare and modified platinum electrode with geometric area of 0.07 cm² was used as working electrode. The platinum electrode was modified through drop casting method [20], where 1 mg of synthesized powder was dispersed ultrasonically in 0.1 mL solvent; acetone to form a suspension. 2 μL was deposited on platinum electrode using

micropipette in the form of thin layer and dried in open air at room temperature for solvent to evaporate. Then, 1 to 2 drops of 5 wt% Nafion (Sigma Aldrich) solution in ethanol were added onto it and dried further in an oven for 5 minutes.

Material Characterization

Powder X-ray diffraction (XRD) patterns of synthesized samples were recorded on an X-ray diffractometer using $\text{CuK}\alpha$ as the radiation source ($\lambda = 1.541 \text{ \AA}$) at room temperature in 2θ range of 20 to 80° . The Fourier transform infrared spectroscopy (FTIR) was used to characterize the final perovskites structured metal oxides. The surface morphology of as synthesized powders was observed by scanning electron microscope (SEM).

Electrochemical Measurements

Electrochemical studies, cyclic voltammetry (CV) have been carried out in three electrode electrochemical cell of 50 mL capacity using Gamry framework version 6. The platinum wire was used as counter and Ag/AgCl (sat'd KCl) was used as reference electrode. CV was carried out between 0.1 V - 0.8 V potential scans in 0.5 M H_2SO_4 with methanol as an analyte. Before recording the final voltammogram, the electrode was cycled for 5 runs at potential scan of 100 mV s^{-1} in acidic medium. Electro-oxidation of methanol was studied by varying temperature (20°C , 25°C , 30°C , 35°C , 40°C , 45°C , 50°C), final concentration of methanol (0.25 M, 0.5 M, 0.75 M, 1.0 M, 1.25 M, 1.5 M, 1.75 M, 2.0 M, 2.25 M) and scan rate of 10 through 1000 mV s^{-1} was used in each separate experiment. The data was averaged over triplicate results.

Results and Discussion

XRD analysis

Fig. 1 presents X-ray diffraction patterns of synthesized BaCeO_3 (BCO) and its zinc doped analogues (BCZO-1, BCZO-8). The XRD pattern of BaCeO_3 is comparable with standard reference card no 00-022-0074 which belongs to orthorhombic structure, Pbnm [21]. All the doped samples ($0.14 \leq x \leq 0.02$) were single perovskite phases and isostructural to pure barium cerate indicating entrance of zinc into lattice instead of accumulation into the grain boundaries [22].

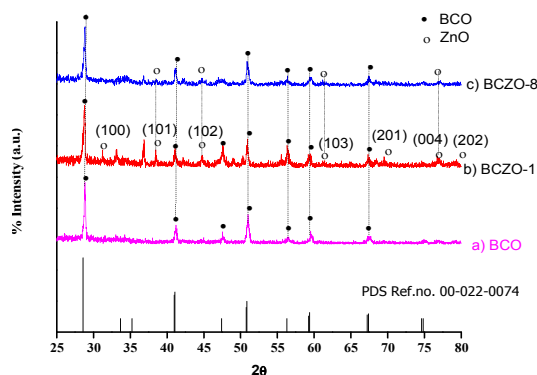


Fig. 1: XRD patterns of a) BCO, b) BCZO-1 and c) BCZO-8 compared with reference.

The average crystallite size was estimated using Scherrer's formula [23-25].

$$D \text{ (nm)} = k \lambda / \beta \cos\theta \quad (1)$$

where D is the average crystallite size in nanometers, k is a constant or shape factor and equal to 0.9, λ is the wavelength of the radiation (0.154 nm), β is the peak width at half maximum intensity and θ is the peak position. The calculated average crystalline size was found in the range of 23-55 nm for all powders.

FTIR Studies

The infrared spectra of BCO and Zn doped powders calcined at 800°C are shown in Fig. 2.

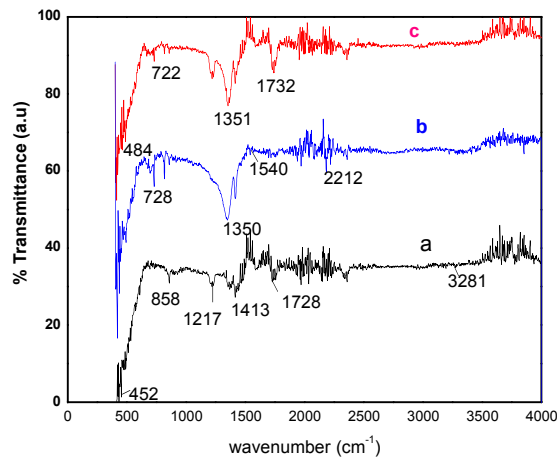


Fig. 2: FTIR spectra of a) BCO, b) BCZO-1, c) BCZO-8.

FTIR of pure BCO (Fig. 2a) exhibited narrow peaks showing maximum interaction of barium and cerium with oxygen. The bands located from 452 cm^{-1} and 858 cm^{-1} indicated the presence of Ce-O vibration and Ba-O vibration, respectively [26, 27].

In FTIR spectra of BCZO-1 (Fig. 2b) and BCZO-8 (Fig. 2c), the broad bands located at 722, 728, 1350, and 1540 cm^{-1} showed the existence of Zn-O vibration [28, 29]. The FTIR of all doped barium cerates were broad indicating the interaction of zinc with oxygen in place of cerium in the perovskite lattice. All other synthesized samples with x from 0.04 to 0.14 showed similar FTIR spectra as that of minimum zinc doped barium cerate. The other bands located between 3000 and 3500 cm^{-1} corresponded to the O-H stretching which could originate from measurement environment.

Cyclic Voltammetric Investigation

To investigate the electrocatalytic activity, the methanol oxidation was studied using cyclic voltammetry in an assembly combining direct methanol fuel cell (DMFC) and PEMFC strategies. The catalyst material was drop-casted onto Pt active area and coated with Nafion (a proton conductor polymer) thus formulating a PEMFC set-up. Methanol was used as the direct fuel (as analyte) for cyclic voltammetric data analysis of its electro-oxidation thus leading to a false-DMFC type of cell testing. The results are presented here for BCO and maximum Zn-doped sample, BCZO-8. The Pt working electrode was modified with BCO or BCZO and kinetic and thermodynamic parameters were evaluated from the effects of scan rates, temperatures and concentration on the voltammetric profiles.

Voltammetric Profiles for Scan Rate Effect

Electrochemical oxidation of methanol was studied while keeping its concentration constant by varying the scan rates from lower values like 10 through 100 to higher value up to 1000 mV s^{-1} on modified Pt working electrode in a positive potential range from 0 to 0.8 V and reversing the scan direction in a cyclic voltammetric manner. The voltammetric profile of methanol oxidation at different scan rates is shown in Fig. 3. All the BCO- and BCZO-modified electrodes could show the stable and steady voltammograms for methanol oxidation under the given set of experimentation.

The diffusion coefficient demonstrates the facility of the diffusion of the analyte towards the working electrode and of the resulting charge transfer process. Thus an estimate of it can lead to an understanding the role of the active material (BCO or BCZO in present case) in the electro-kinetics of the analyte. To calculate the diffusion coefficient for methanol redox system, the Randles-Sevcik equation was used [20]:

$$I_p = 2.99 \times 10^5 n(n\alpha)^{1/2} A C D_0^{1/2} \nu^{1/2} \quad (2)$$

In this equation, I_p is the peak current (A), ν is the scan rate (V s^{-1}), C is the concentration (mol cm^{-3}), A is the area of electrode (cm^2) while D_0 is the diffusion coefficient in $\text{cm}^2 \text{s}^{-1}$. From the slope of plot of I_p vs. $\nu^{1/2}$, D_0 was calculated.

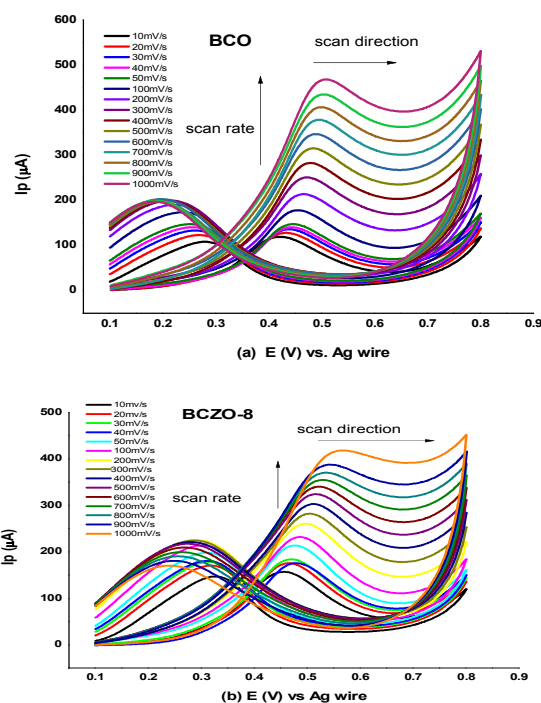


Fig. 3: Cyclic voltammograms for 2 M CH_3OH on platinum electrodes modified with a) BCO and b) BCZO-8 in 0.5 M H_2SO_4 at scan rates of 10 to 1000 mVs^{-1} .

The potential of BCO and its doped analogues is demonstrated in the facile kinetic parameter that is the higher peak currents with the scan rates (Fig. 4a) and the resultant diffusion coefficient. The diffusion coefficient of methanol was found to be $1.44 \times 10^{-10} \text{ cm}^2 \text{ s}^{-1}$ and $7.16 \times 10^{-11} \text{ cm}^2 \text{ s}^{-1}$ using BCO and BCZO-8 modified electrodes, respectively. The obtained values in this study were found to be more than literature reported value (in order of $10^{-12} \text{ cm}^2 \text{ s}^{-1}$) [30]. Zinc doping is manifested in the mechanical and chemical stability of the BCO samples as these were found stable in an environment of acidic oxidation of methanol and the temperature effect up to 50 $^\circ\text{C}$ could not disturb the measurement system. The electrooxidation of methanol was facilitated using the zinc doped barium cerates which are the advanced materials for future technologies such as fuel cells. The higher diffusion coefficient of methanol using BCO could be due to

the availability of more active sites at BCO-modified platinum electrode for adsorbed species to oxidize into CO_2 in comparison to zinc doped samples.

Voltammetric Profiles for Concentration Effect

To investigate the effect of methanol concentration on its electro-oxidation, cyclic voltammograms were taken at 100 mV s^{-1} . Fig. 4 represents the effect of methanol concentration on its voltammetric profile using BCO modified Pt electrode. One could see the increase in peak current with the increase in methanol concentration (up to 2 M). However, on increasing the concentration of methanol beyond 2 M, the peak current was decreased. The result could be attributed to the blocking of the electrode sites due to more adsorbed intermediates which then inhibit the oxidation of methanol [4, 31]. The reverse scans also showed enhanced peak currents with methanol concentration which case may be attributed to the fast and feasible oxidation of the adsorbed CO type species [32]. Overall redox processes seemed to be diffusion controlled and facilitated due to the proton conducting nature of doped or undoped barium cerate materials [6, 7].

Similar results were obtained for BCZO-8 modified electrode, however the peak current obtained was a little less as compared to that for BCO modified electrode as could be seen from the graph showing comparative peak currents (Fig. 4b).

The catalytic properties of the materials can be invoked by observing the heterogeneous kinetics involved in the redox processes. The suitability of the synthesized barium cerates was probed for the electro-oxidation of methanol. The better value of the standard heterogeneous rate constant manifests the facilitated electron transfer process and it would demonstrate the electrode material activity that is catalysis. Reinmuth equation was used to estimate the standard heterogeneous rate constant, k_{sh} [33]:

$$I_p = n F A C k_{sh} \quad (3)$$

In this equation, k_{sh} is the heterogeneous rate constant while F is the Faraday's constant. Using Reinmuth plots, the value of rate constant, k_{sh} for methanol oxidation could be obtained from the slopes of the linear graphs between I_p and methanol concentration as $0.45 \times 10^{-5} \text{ cm}^2 \text{ s}^{-1}$ and $0.51 \times 10^{-5} \text{ cm}^2 \text{ s}^{-1}$ using BCO and BCZO-8 modified Pt electrodes, respectively, Fig. 5:

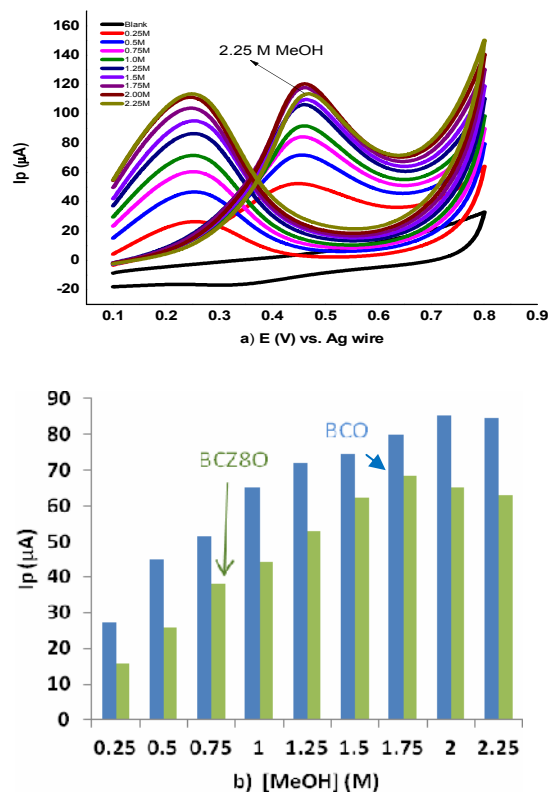


Fig. 4: Cyclic voltammograms for methanol oxidation using BCO at scan rate of 100 mV s^{-1} in $0.5 \text{ M H}_2\text{SO}_4$ at 298 K , b) Comparative peak currents for methanol oxidation using BCO and BCZO-8.

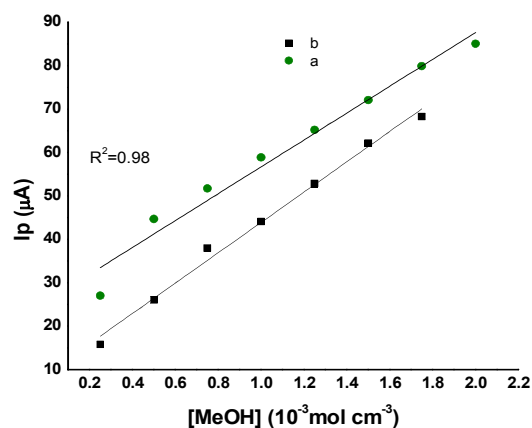


Fig. 5: Reinmuth plots of I_p (μA) vs. methanol concentration (mol cm^{-3}) using a) BCO b) BCZO-8 modified Pt electrodes.

Although the rate constants are close to each other using either of the modified electrodes, the facile kinetics was obvious for the electro-oxidation of methanol which is the direct fuel source for

PEMFC technology. These results demonstrated the suitability of the BCO and BCZO materials as electrocatalysts.

Voltammetric Profiles for Temperature Effect

The voltammetric profiles of the electro-oxidation of methanol were also observed in a low temperature range, from 25 to 50 °C which is a working range for PEMFCs. The increasing temperature was found to cause a significant increase in the anodic peak current in all the systems (only two samples are shown here). This indicated that the increasing temperature can enhance the rate of electro-oxidation of methanol by facilitating faster electron transfer.

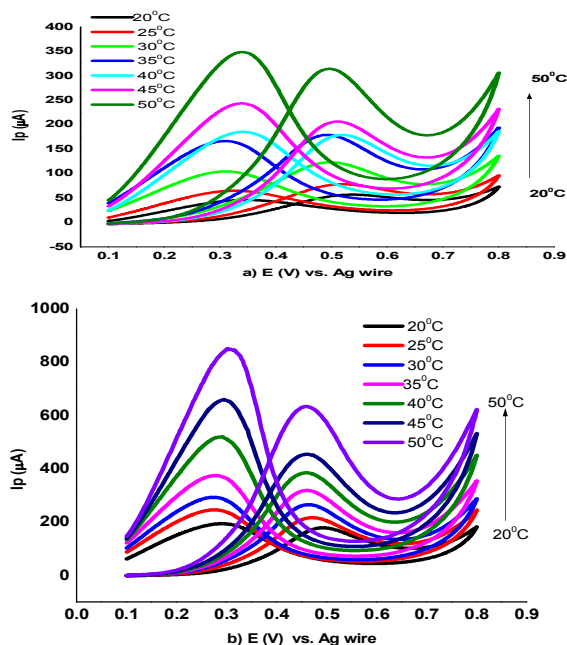


Fig. 6: Voltammograms for methanol oxidation using a) BCO b) BCZO-8 at various temperatures.

Fig. 6 shows the temperature dependence of methanol oxidation using modified electrodes. From the temperature variation study, we can deduce that the electro-oxidation is facilitated with increasing temperature and the cell system remains stable in acidic medium. The fortifying back current in these CV profiles also manifested the occurrence of various electrochemical reactions at the electrodes which produce many intermediate species that block the active site of electrode surface when adsorbed. The intermediate species formed in methanol oxidation process can be removed and/or desorbed by increasing temperature providing fresh surface which can contribute to the enhancement of peak current.

Moreover, this pronounced EC behaviour can also be attributed to decrease in viscosity (thus more diffusion) at higher temperature. The temperature variation in low temperature range under the given set of experimental conditions, again hints clearly towards the effectiveness of the barium cerate materials for PEMFC applications.

Arrhenius plots of logarithm of heterogeneous rate constant (k_s) versus the reciprocal of temperature (T^{-1}) provided the apparent activation energy, E_a , Fig. 7.

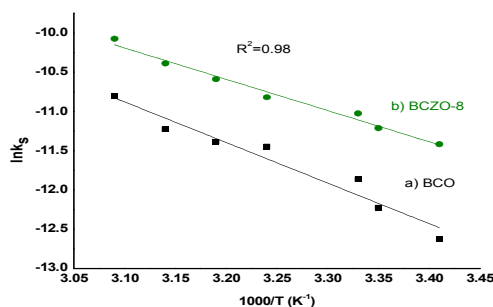


Fig. 7: Arrhenius plots for methanol oxidation at platinum electrodes modified with a) BCO and b) BCZO-8.

Activation energies for the electro-oxidation of methanol were found to be 0.44 eV and 0.34 eV using BCO and BCZO materials as electrocatalysts, respectively. The low value of E_a in case of BCZO-8 can be correlated to the high values of peak currents obtained in this case (compare Fig. 6a and 6b). The increase in peak current with temperature on BCO or BCZO modified electrodes manifests an enhanced conductive behavior and finds application in intermediate temperature fuel cells.

Evaluation of Thermodynamic Parameters

Different thermodynamic parameters were also deduced for the electro-oxidation of methanol using BCO and BCZO materials as electrocatalysts, with the help of Marcus equation [34–38]:

$$k_s = Z_{het} \exp \left[\frac{-\Delta G^\ddagger}{RT} \right] \quad (4)$$

where ΔG^\ddagger the free energy of activation is, Z_{het} is the collision number while R and T have usual significance.

Z_{het} at various temperatures can be derived using the following equation.

$$Z_{het} = \left(\frac{RT}{2\pi M} \right)^{1/2} \quad (5)$$

In above equation, M stands for the molar mass of the analyte (methanol in this case). Equation 3 can be re-arranged as

$$\ln\left(\frac{k_s}{Z_{het}}\right) = \frac{-\Delta G^\ddagger}{RT} \quad (6)$$

We know that

$$\Delta G^\ddagger = \Delta H^\ddagger - T \Delta S^\ddagger \quad (7)$$

Substituting for ΔG^\ddagger using eq. 7, the eq. 6 takes the form:

$$\ln\left(\frac{k_s}{Z_{het}}\right) = \frac{-\Delta H^\ddagger}{RT} + \frac{\Delta S^\ddagger}{R} \quad (8)$$

Equation 8 is a straight line equation and gives value of ΔH^\ddagger from the slope of the plot of $\ln[k_s/Z_{het}]$ vs. $1/T$ while ΔS^\ddagger can be estimated from the intercept. The respective plots are shown in Fig. 8 for the electro-oxidation of methanol using both BCO and BCZO modified Pt electrodes. The obtained values of ΔH^\ddagger , ΔS^\ddagger , and ΔG^\ddagger , are tabulated in Table 1.

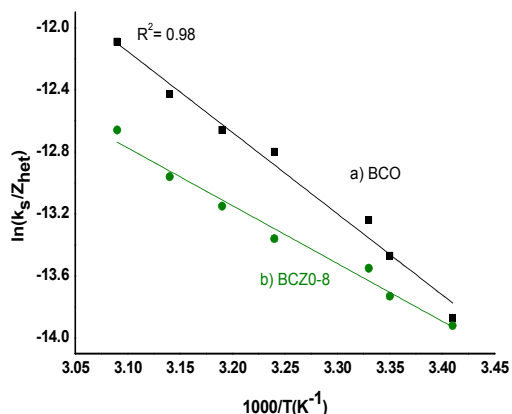


Fig. 8: Functional plots of $\ln(k_s/Z_{het})$ vs. $1/T$ for electro-oxidation of 2 M methanol at modified platinum electrode with; a) BCO and b) BCZO-8.

Table-1: Thermodynamic data for the electro-oxidation of methanol on modified electrodes.

Modified Electrodes	ΔH^\ddagger (kJ mol ⁻¹)	ΔS^\ddagger (J mol ⁻¹ K ⁻¹)	ΔG^\ddagger (kJ mol ⁻¹)
BCO/Pt	43.48	33.75	32.58
BCZO-8/Pt	30.94	-10.30	34.27

The observed positive values of ΔG^\ddagger , show the electro-oxidation of methanol to be non-spontaneous and endothermic in all cases.

Morphological Investigation

SEM analysis of calcined powders of BCO, BCZO-1, BCZO-3, and BCZO-8 synthesized by co-precipitation method was carried out at different resolutions to study their morphology.

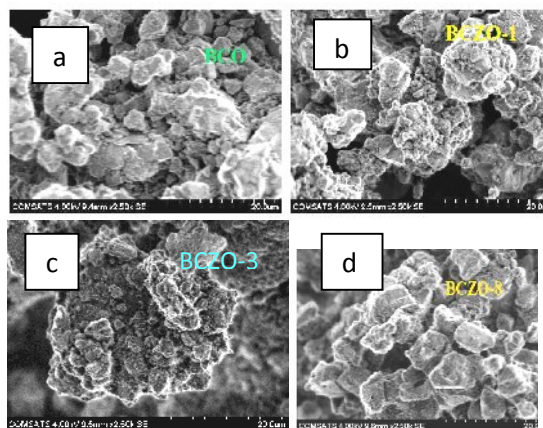


Fig. 9: SEM images of a) BCO b) BCZO-1 c) BCZO-3 d) BCZO-8 at 20 nm resolution.

The SEM morphological studies of synthesized powders showed fine homogeneity. From these images, it was also confirmed that BCO, BCZO-1, BCZO-3 had less porosity (and more density) and less agglomeration of particles compared to that of BCZO-8. At zinc doping level of 16 mol% (BCZO-8), ZnO may have formed additional grain boundaries as also indicated by more porosity.

Conclusion

Barium cerate and zinc doped barium cerates of different zinc contents were prepared by co-precipitation method and investigated by using XRD, SEM, FTIR techniques and catalytic activity towards methanol oxidation in acidic medium was done by using cyclic voltammetry. The effect of dopant incorporation into perovskite lattice of the calcined powder was studied. SEM images displayed fine homogeneity of the particles. With increase in concentration of zinc, agglomeration occurred. A single orthorhombic phase perovskite was obtained for BaCeO₃ (BCO) indicated by XRD. The electrochemical oxidation of methanol by modifying Pt electrode with BCO and BCZO-8 was found to be irreversible giving only anodic peaks at 0.4 – 0.5 V. The current increased almost 10 times on increasing scan rate from 100 to 1000 mV s⁻¹ with multistep followed by re-oxidation of the adsorbed intermediate species on the working electrode. The shift in potential from more positive to less positive ensured the irreversibility of methanol oxidation. The diffusion coefficient for methanol oxidation using

BaCeO₃ was higher as compared to zinc doped BaCe_{1-x}Zn_xO₃ due to comparative more availability of active sites for adsorption of intermediate species on the modified platinum electrode. The increasing temperature and analyte concentration (up to 2 M) increased peak current due to more diffusion and enhancement in electro-oxidation rate. The methanol oxidation assembly was stable over the entire methanol concentration, the scan rates, and the working temperature range. This study is the first time report for such an application of the perovskite materials in PEMFC conditions. The cell stability and resulting catalytic activity of the used perovskite materials pointed strongly to their potentiality as electrode materials in fuel cell technologies [6, 18, 22, 39-41].

Acknowledgement

The corresponding author is thankful to Quaid-i-Azam University Islamabad for experimental facilities and HEC for the Project# 20-1718/R & D/2010 (Gamry workstation).

References

1. E. Pallotti, F. Mangiatordi, M. Fasano and P. Del Vecchio, in Environment and Electrical Engineering (EEEIC), *12th International Conference on IEEE*, p. 440 (2013).
2. F. H. Soriano and F. Mulatero, EU Research and Innovation (R&I) in Renewable Energies: The Role of the Strategic Energy Technology Plan (SET-Plan), *Energy Policy*, **39**, 3582 (2011).
3. J. M. Zen, A. S. Kumar and D. M. Tsai, Recent Updates of Chemically Modified Electrodes in Analytical Chemistry, *Electroanalysis*, **15**, 1073 (2003).
4. W. Z. Zhu and S. C. Deevi, A Review on the Status of Anode Materials for Solid Oxide Fuel Cells, *Mater. Sci. Eng.*, **A362**, 228 (2003).
5. J. H. Xu, J. Xiang, H. Ding, T. Q. Yu, J. Le Li, Z. G. Li, Y. W. Yang and X. L. Shao, Synthesis and Electrical Properties of BaCeO₃-Based Proton Conductors by Calcinations of Metal-Polyvinyl Alcohol Gel, *J. Alloys Comp.*, **551**, 333 (2013).
6. D. Medvedev, A. Murashkina, E. Pikalova, A. Demin, A. Podias and P. Tsiakaras, BaCeO₃: Materials Development, Properties and Application, *Prog. Mater. Sci.*, **60**, 72 (2014).
7. A. K. Azad, A. Kruth and J. T. S. Irvine, Influence of Atmosphere on Redox Structure of BaCe_{0.9}Y_{0.1}O_{2.95-δ} Insight from Neutron Diffraction Study, *Int. J. Hyd. Energy*, **39**, 12804 (2014).
8. K. H. Ryu and S. M. Haile, Chemical Stability and Proton Conductivity of Doped BaCeO₃-BaZrO₃ Solid Solutions, *Solid State Ionics*, **125**, 355 (1999).
9. Z. Shao, W. Zhou and Z. Zhu, Advanced Synthesis of Materials for Intermediate-Temperature Solid Oxide Fuel Cells, *Prog. Mater. Sci.*, **57**, 804 (2012).
10. F. Chen, O. T. Sorensen, G. Y. Meng and D. Peng, Thermal Decomposition of BaC₂O₄.0.5H₂O Studied by Stepwise Isothermal Analysis and Non-Isothermal Thermogravimetry, *J. Therm. Analysis Calor.*, **53**, 397 (1998).
11. S. B. Boskovic, B. Z. Matovic, M. D. Vljajic and V. D. Kristic, Modified Glycine Nitrate Procedure (MGNP) for the Synthesis of SOFC Nanopowders, *Ceram. Inter.*, **33**, 89 (2007).
12. C. S. Tu, C. C. Huang, S. Lee, R. Chien, V. Schmid and C. L. Tsai, Effect of Lithium Fluoride on Thermal Stability of Proton-Conducting Ba (Zr_{0.8-x}Ce_xY_{0.2}) O_{2.9} Ceramics, *Solid State Ionics*, **181**, 1654 (2010).
13. A. Orlov, O. Shlyakhtin, A. Vinokurov, A. Knotko and Y. D. Tret'yakov, Preparation and Properties of Fine BaCeO₃ Powders for Low-Temperature Sintering, *Inorg. Mat.*, **41**, 1194 (2005).
14. S. D. Flint and R. C. T. Slade, Variations in Ionic Conductivity of Calcium-Doped Barium Cerate Ceramic Electrolytes in Different Atmospheres, *Solid State Ionics*, **77**, 215 (1995).
15. E. A. Batista, R. P. Malpass, A. J. Motheo and T. Iwasita, New Mechanistic Aspects of Methanol Oxidation, *J. Electroanal. Chem.*, **571**, 273 (2004).
16. J. P. P. Huijsmans, F. P. F. Berkel and G. M. Christie, Intermediate Temperature SOFC—a Promise for the 21st century, *J. Power Sources*, **71**, 107 (1998).
17. O. A. Hazzazi, G. A. Attard, P. B. Wells, F. J. Vidal-Iglesias and M. Casadesus, Electrochemical Characterization of Gold on Pt{hkl} for Ethanol Electrocatalysis, *J. Electroanal. Chem.*, **625**, 123 (2009).
18. A. Maksic, Z. Rakocevic, M. Smiljanic, M. Nenadovic and S. Strbac, Methanol Oxidation on Pd/Pt (poly) in Alkaline Solution, *J. Power Sources*, **273**, 724 (2015).
19. L. A. García, C. Ramírez, J. M. H. Lopez and E. M. A. Estrada, Electrocatalytic Activity of

- Nanosized Pt Alloys in the Methanol Oxidation Reaction, *J. Alloys Comp.*, **495**, 462 (2010).
20. A. Mujtaba and N. K. Janjua, Fabrication and Electrocatalytic Application of CuO@Al₂O₃ Hybrids, *J. Electrochem. Soc.*, **162**, H328 (2015).
 21. K. S. Knight and N. Bonanos, The Crystal Structures of Some Doped and Undoped Alkaline Earth Cerate Perovskites, *Materials Research Bulletin*, **30**, 347 (1995).
 22. D. Medvedev, J. Lyagaeva, S. Plaksin, A. Demin and P. Tsiakaras, Sulfur and Carbon Tolerance of BaCeO₃-BaZrO₃ Proton-Conducting Materials, *J. Power Sources*, **273**, 716 (2015).
 23. Y. W. Wang, L. D. Zhang, G. Z. Wang, X. S. Peng, Z. Q. Chu and C. H. Liang, Catalytic Growth of Semiconducting Zinc Oxide Nanowires and their Photoluminescence Properties, *J. Cryst. Growth*, **234**, 171 (2002).
 24. A. K. Azad and J. T. S. Irvine, High Density and Low Temperature Sintered Proton Conductor BaCe_{0.5}Zr_{0.35}Sc_{0.1}Zn_{0.05}O_{3-δ}, *Solid State Ionics*, **179**, 678 (2008).
 25. A. Peterson, The Scherrer Formula for X-Ray Particle Size Determination, *Phys. Rev.*, **10**, 978 (1939).
 26. J. S. S. J. Ketzial, D. Radhika and A. S. Nesaraj, Low-Temperature Preparation and Physical Characterization of Doped BaCeO₃ Nanoparticles by Chemical Precipitation, *Int. J. Indus. Chem.*, **4**, 18 (2013).
 27. P. Pasierb, S. Komornicki, M. Rokita and M. Rekas, Structural Properties of Li₂CO₃-BaCO₃ System Derived from IR and Raman Spectroscopy, *J. Mol. Struct.*, **596**, 151 (2001).
 28. H. C. Gupta, P. Simon, T. Pagnier and G. Lucazeau, Force Constant Calculation from Raman and IR Spectra in the Three Non-Cubic Phases of BaCeO₃, *J. Raman Spec.*, **32**, 331 (2001).
 29. J. Singh, P. Kumar, K. S. Hui, K. N. Hui, K. Ramam, R. S. Tiwari and O. N. Srivastava, Synthesis, Band-Gap Tuning, Structural and Optical Investigations of Mg Doped ZnO Nanowires, *J. Cryst. Eng. Comm.*, **14**, 5898 (2012).
 30. G. Hou, J. Parrondo, V. Ramani and J. Prakash, Kinetic and Mechanistic Investigation of Methanol Oxidation on a Smooth Polycrystalline Pt Surface, *J. Electrochem. Soc.*, **161**, F252 (2014).
 31. R. Parsons and T. VanderNoot, The Oxidation of Small Organic Molecules: a Survey of Recent Fuel Cell Related Research, *J. Electroanal. Chem.*, **257**, 9 (1988).
 32. T. Iwasita, Electrocatalysis of Methanol Oxidation, *Electrochim. Acta*, **47**, 3663 (2002).
 33. R. Awasthi and R. N. Singh, Optimization of the Pd-Sn-GNS Nanocomposite for Enhanced Electrooxidation of Methanol, *Int. J. Hyd. Energy*, **37**, 2103 (2012).
 34. R. S. Nicholson and I. Shain, Theory of Stationary Electrode Polarography. Single Scan and Cyclic Methods Applied to Reversible, Irreversible, and Kinetic Systems, *Anal. Chem.*, **36**, 706 (1964).
 35. I. I. Naqvi, M. Z. Kirmani, R. Parveen, M. Nazir and M. Ashfaq, Evaluation of Kinetic and Thermodynamic Parameters of 1, 1'-Dibenzoylferrocene in Methanol by Cyclic Voltammetry, *J. Chem. Soc. Pak.*, **2**, 183 (2012).
 36. A. S. A. Khan, R. Ahmed and M. L. Mirza, Evaluation of Catalytic Activity of Pt and Pt-Ru Catalysts for Electro-Oxidation of Methanol in Acid Medium by Cyclic Voltammetry, *Portug. Electrochim. Acta*, **27**, 429 (2009).
 37. A. S. A. Khan, R. Ahmed and M. L. Mirza, Electro-oxidation of Methanol on Fuel Cell Catalysts and Evaluation of their Catalytic Activities by Cyclic Voltammetry, *J. Chem. Soc. Pak.*, **30**, 810 (2008).
 38. R. A. Marcus, Electron Transfer Reactions in Chemistry. Theory and Experiment, *Rev. Modern Phys.*, **65**, 599 (1993).
 39. Z. Gao, R. Raza, B. Zhu and Z. Mao, Development of Methanol-fueled Low-Temperature Solid Oxide Fuel Cells, *Int. J. Energy Res.*, **35**, 690 (2011).
 40. A. Radojković, S. M. Savić, N. Jović, J. Ćirković, Ž. Despotović, A. Ribić, Z. Branković and G. Branković, Structural and Electrical Properties of BaCe_{0.9}Ee_{0.1}O_{2.95} Electrolyte for IT-SOFCs, *Electrochim. Acta*, **161**, 153 (2015).
 41. A. Lacz, K. Grzesik and P. Pasierb, Electrical Properties of BaCeO₃-Based Composite Protonic Conductors, *J. Power Sources*, **279**, 80 (2015).